Preliminary Study on Machining of Additively Manufactured Ti-6Al-4V

Jay K. Raval[1], Aamer A. Kazi[1], Xiangyu Guo[1], Ryan Zvanut[2], Chabum Lee[1], Bruce L. Tai[1]

[1] Department of Mechanical Engineering, Texas A&M University, College Station, TX, 77840

[2] Kansas City National Security Campus, Honeywell FM&T, Kansas City, MO, 64147

Abstract

Additively manufactured metals differ from their conventionally produced counterparts due to the inherent material inhomogeneity, porosity, and thermal stress induced by the process. These differences make the machining of additively manufactured metals more difficult and cause premature tool failure or unexpected surface finish at certain conditions. This study takes the first step to investigate and identify the causes of these issues, particularly for Ti-6Al-4V. Printed and wrought samples, as well as heat treatment effect, are compared in a dry cutting condition at a cutting speed of 90 m/min in terms of cutting power, vibration, temperature, and produced surface finish. The results show a lower cutting power and more vibration for as-printed Ti samples, indicating a less ductile microstructure and inclusion of pores. Heat treatment can eliminate these phenomena. There is no significant difference found in the produced surface finish at the current cutting condition.

Keywords: Titanium, Ti-6-4, Additive Manufacturing, Machinability

1. Introduction

Titanium (Ti) alloys are engineering materials that are widely used for their high corrosion resistance, biocompatibility and strength-to-weight ratio, the highest of any metallic element [1]. It finds applications in industries ranging from dentistry to aerospace [2]. Accounting for more than 50% of all Ti alloy usage, Ti-6Al-4V is currently the most widely used alloy due to its dual (α)-(β) microstructure [3]. Given its importance in the engineering industry, researchers have taken to studying the additive manufacturability (AM) of the alloy. Several AM processes have been used to successfully manufacture titanium, such as Selective Laser Sintering (SLS), Selective Laser Melting (SLM), Direct Energy Deposition (DED) and Electron Beam Melting (EBM) [4]. Further advancements in these technologies will allow the industry to reduce material wastage, cut costs and improve efficiency [5].

The freeform ability of AM technologies has allowed the creation of complex part geometries [6]. Unlike the traditional manufacturing process, in AM process, the layer-by-layer building of the 3D geometry involves multiple rapid heating and cooling cycles on the part. These thermal cycling can generate porosity, residual stress and warpage in the manufactured part. While porosity and residual stresses can be alleviated by stress relieving, tolerances and surface profile can only be improved by machining processes [7,8]. Research shows that there are inherent differences in microstructure and mechanical properties between wrought and AM parts [9]. As a result, traditional machining parameters optimized for wrought metals may or may not be optimum for AM parts [10]. Hence, there is a need to identify these differences and investigate the factors responsible for them.

The objective of this paper is to study and quantify the differences observed when machining wrought and AM Ti and those with additional stress relief heat treatment. This is done by performing orthogonal turning tests on a CNC lathe. A dry cutting condition was used to amplify the inherent differences between wrought and AM samples. These differences are observed by measuring and monitoring cutting power and acceleration (vibration) during machining. Cutting power provides steady state cutting force, while an accelerometer can capture a wide range of vibration frequencies (up to 10-15 kHz). This is aimed to include more cutting information than that from single dynamometer measurement, for example, the material inhomogeneity and porosity. In addition, cutting temperature is also monitored during a cut. Temperature is an important outcome to be considered while machining titanium. Titanium has a low thermal conductivity of about 7 W/m K, and this can create high cutting zone temperatures, which may have detrimental effects on the cutting tool [11]. This can affect the finished surfaces differently for wrought and AM titanium. Finally, produced surface roughness is used to validate the quality of the final machined part.

To structure this paper, section 2 describes the setup and methodologies, describing the experimental design and the measurement methodology for each parameter. Section 3 describes the individual results obtained for each parameter. Section 4 discusses the results and section 5 concludes the paper.

2. Setup and Methodologies

This section describes the experiment design and the equipment and principles used for measurement. Cutting power, vibrations, cutting zone temperature, and surface roughness of the machined surface are used to quantify the machinability of the materials.

2.1 Experiment Design

The tests include machining of four different types of material conditions: wrought Ti-6Al-4V (Ti-W), wrought stress relieved Ti-6AL-4V (Ti-W-SR), additively manufactured Ti-6AL-4V (Ti-AM) and additively manufactured stress relieved Ti-6AL-4V (Ti-AM-SR). All samples were prepared and provided by Kansas City National Security Campus (KCNSC). Additively manufactured samples were made using a selective laser sintering (SLS) process on an EOS M290 system (Munich, Germany) with the default parameters for printing Ti-6AL-4V. Ti-W-SR and Ti-AM-SR samples went through the same stress relief heat treatment by heating at 800°C for four hours.

The turning experiments were conducted on an EMCO (Hallein, Austria) CT60 CNC lathe. The cutting setup is shown in Fig. 1. A combination of power cell and accelerometer is used to monitor the steady state cutting power and dynamic vibrations during cutting, respectively. The in-situ cutting zone temperature was measured using the tool-workpiece thermocouple method. All the cutting tests were performed dry at a cutting speed of 90 m/min, with a feed rate of 0.05 mm/rev and 0.25 mm depth of cut for a finish process. A new Kennametal DCGT070201LF type insert with a nose radius of 0.1 mm was used for each test. The insert was oriented such that the major cutting-edge angle is about 95 degrees. These cutting conditions were based upon commonly used values by the industry. It is to be noted that dry machining is rarely used in the industry for obvious reasons; however, in this study, it is selected to expedite the effects of cutting conditions.

Three repeated tests were performed for each material to check for repeatability and increase the robustness of the results.

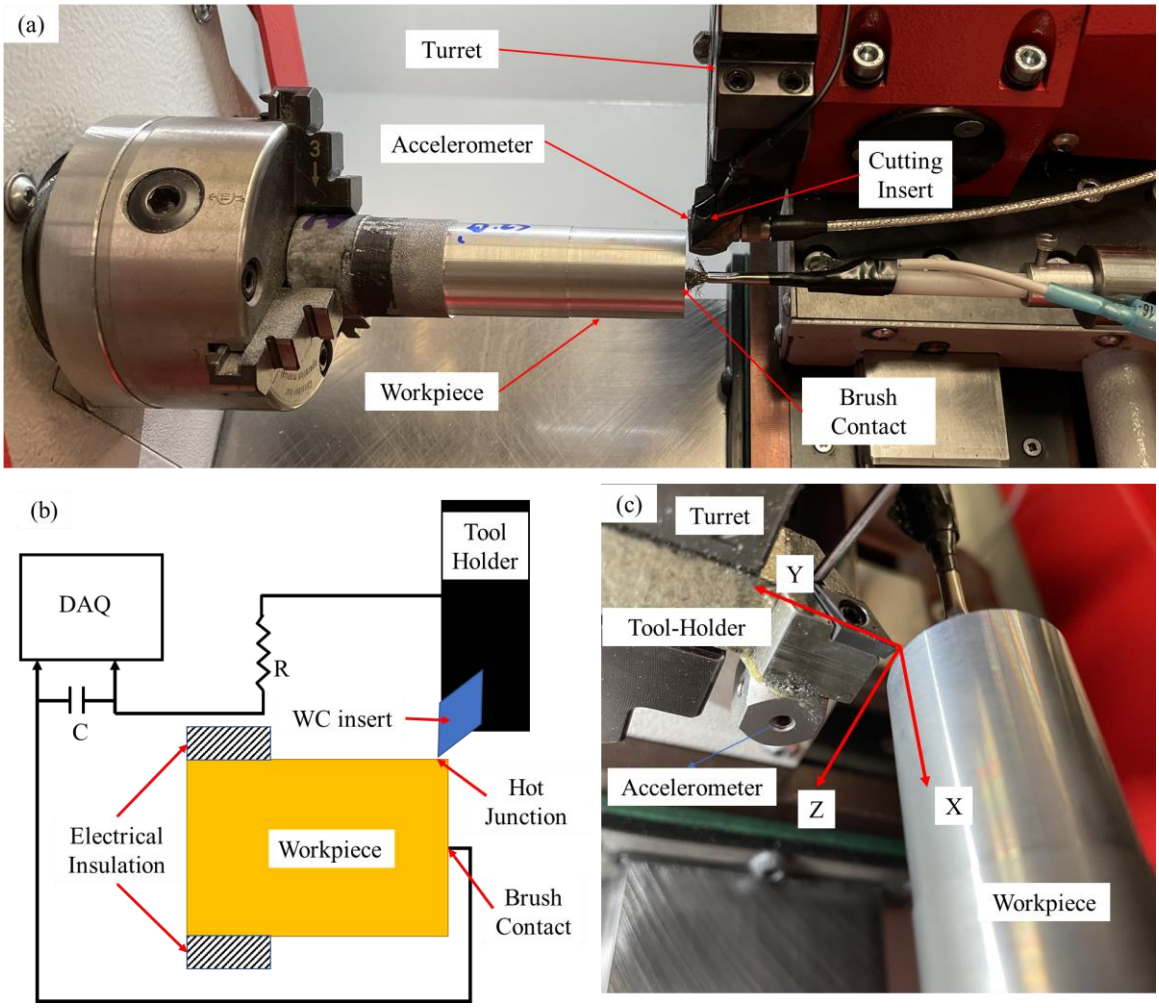

Fig. 1: (a) Image of the experimental setup (b) Schematic of tool-workpiece thermo-emf measurement circuit (c) Vibration measurement setup using accelerometer

2.2 Cutting Power Measurement

The cutting power was monitored by measuring the total power consumed by the spindle using a 3-phase hall effect sensor by Load Controls Inc (Sturbridge, MA). Fig. 2 shows a sample plot of spindle power as a function of time. The spindle power was sampled at 50 Hz using NI 6341 USB DAQ. The initial spike in power is when the spindle is turned on. The power settles down to a constant value as soon as constant RPM has been achieved, which is termed as idle power. Idle power includes the power required by the spindle to stay in motion and will change slightly depending on the weight of the workpiece. Once the tool engages into cutting, an increase in the spindle power is seen. This power is termed as the total spindle power which includes the idle power as well as the power required for cutting. Therefore, the idle power is subtracted from the total spindle power to obtain the cutting power. The cutting power is a summation of the power needed to perform cutting as well as the power needed to overcome the friction between the cutting

tool and the workpiece. The cutting power represents an average cutting force under a constant cutting speed (i.e., power = speed × force).

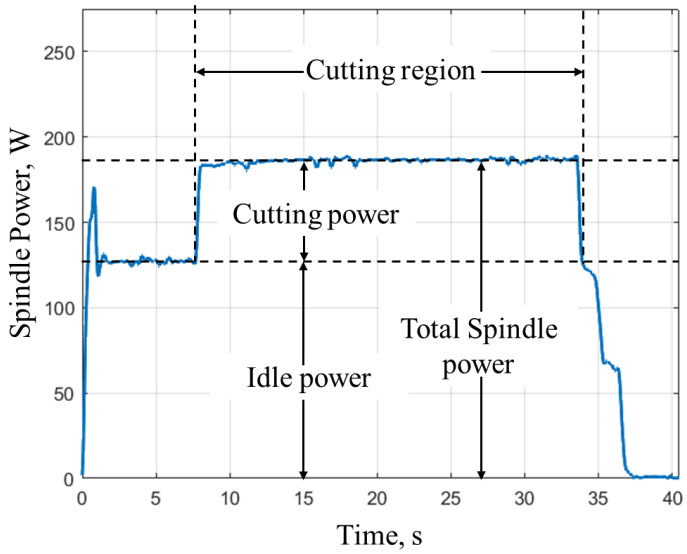

Fig. 2: Typical power consumption of the machine tool spindle

2.3 Vibration Measurement

A Kistler type 8763B ceramic shear accelerometer was attached to the tool holder directly below the cutting edge of the insert, as shown in Fig. 1(b). Even though the accelerometer cannot provide the dynamic force magnitudes, it was still chosen because of its faster response time and minimum effect on the machine's natural frequency (because of its small volume and weight). The accelerometer can capture frequency up to 15 kHz while the dynamometer is typically limited up to 5 kHz. Although the current setup may not provide the dynamic force magnitude, it will provide a wider frequency range of dynamic events as a function of acceleration, which is proportional to the dynamic force acting on the tool. Vibrations in the z-direction (parallel to the cutting direction) were analyzed in this study. Fig. 3 shows a sample accelerometer output obtained during a cutting test. The data was collected at a sampling rate of 10 kHz using a Kistler LabAmp charge amplifier

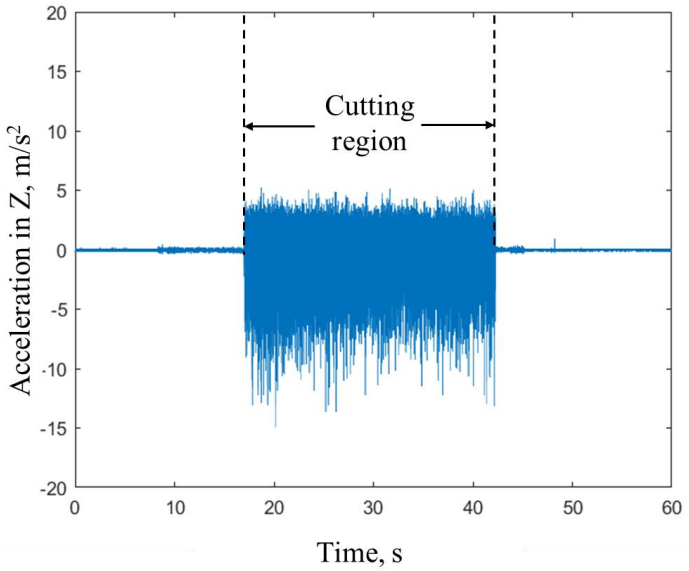

Fig. 3: Typical accelerometer response measured during a test

DAQ. The root-mean-square (rms) value of a vibration profile in the cutting region is used to represent the magnitude of dynamic response.

2.4 Cutting Zone Temperature Measurement

The cutting zone temperature is measured using the tool-workpiece thermocouple technique. This method overcomes the limitations of sensor response time, resolution, and access to the target zones of other available techniques. It utilizes the thermoelectric principle to measure the temperature at the contact surface. The contact between the tool and the workpiece acts as the hot thermocouple junction, while all other contacts across the circuit act as the cold junction. Because of the heat generation at the cutting zone, a thermo-electromotive force (emf) is generated at the hot junction which is measured using the NI USB 6341 DAQ at a sampling rate of 50 Hz. Furthermore, since there is no heat generation at the cold junctions, they will not generate any thermo-emf and therefore will not contribute to the signal generated. However, in order for this method to work, some precautionary measures need to be taken, as explained by Stephenson [12].

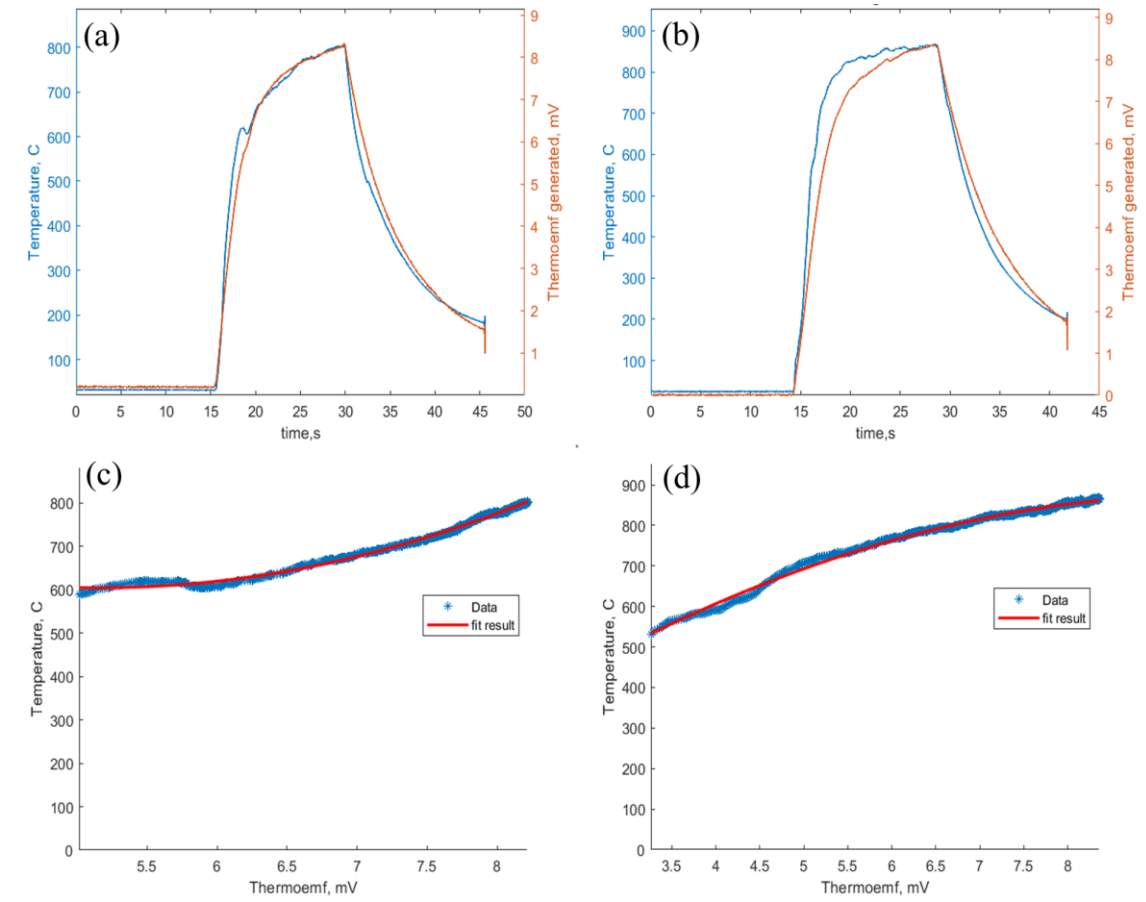

Fig. 4: (a) Thermoemf generated and interface temperature during heating for AM sample (b) Thermoemf generated and interface temperature during heating for wrought sample (c) Calibration curve for AM sample (d) Calibration curve for wrought sample

At least one of the tool or the workpiece (preferably both) needs to be electrically insulated from the rest of the machine and therefore mitigating parallel circuits in the voltage measurement.

For the current setup, the workpiece as well as the tool were electrically insulated from the machine using ceramic paint insulation and mica sheet insulation, respectively. And secondly, because of the use of inserts instead of a solid tool, there are secondary junctions present in the tool holder, so the cutting time needs to be kept short in order to avoid measurement errors due to heat conduction to secondary junctions. Furthermore, a calibration is required to convert the thermo-emf into temperature. To perform the calibration, a tungsten carbide rod, which is the same material as the cutting insert was used to represent the cutting tool. The rod was brazed to the workpiece, and a thermocouple was kept at the junction. The junction was heated using a propane torch and the temperature from the thermocouple and the thermo-emf from the junction were measured to generate the calibration curve shown in Fig. 4. A second-order polynomial fit was used for both cases. Only the high-temperature data (550– 870°C for wrought parts and 600-800 °C for AM parts) was used to generate the calibration curve since the cutting temperatures are expected to be in that range.

2.5 Surface Roughness

The surface roughness (Ra) was measured using a Mitutoyo SJ-210 profilometer. Each workpiece was scanned at three different random locations along the feed direction (i.e., across tooling marks) and data were averaged to obtain the value for the sample. Ra values for all the samples of the same material were than averaged to obtain the characteristic value for that material.

3. Results

3.1 Cutting Power Results

The cutting powers measured using the power cell are summarized in this section. Fig. 5 shows the results obtained. The error bars represent one standard deviation from the mean value of three repetitions. Overall, the wrought part (Ti-W) has the highest cutting power, while the as-

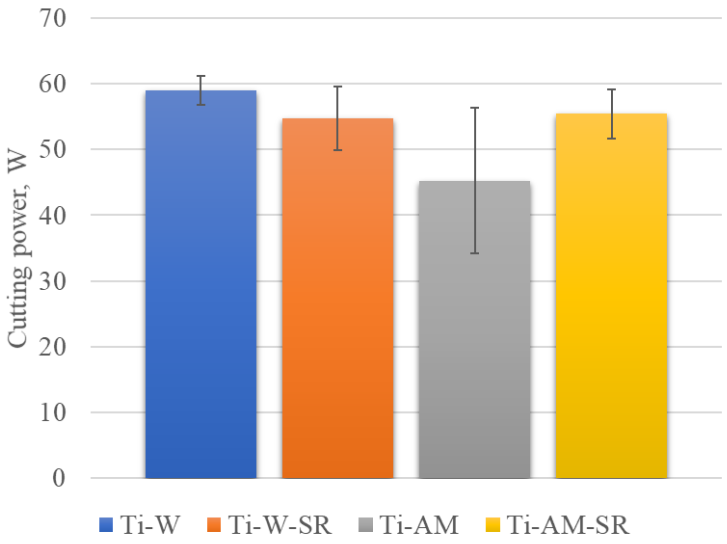

Fig. 5: Steady state cutting power results

printed part (Ti-AM) has the lowest. This indicates a clear material difference between the two manufacturing conditions. Also, the wrought material has provided the most consistent value (i.e., the smallest deviation), while the as-printed AM parts (Ti-AM) tend to show more variability in the machining power between different samples. AM parts after stress relief heat treatment show improved repeatability, as seen by a reduction in the standard deviation from Ti-AM to Ti-AM-SR. The heat treatment also increases the cutting power to reach a similar level to that of Ti-W-SR and Ti-W. As seen, the stress-relief process has a significant impact on the AM parts but not on the wrought parts.

3.2 Vibration Results

The results of vibration measurement are shown in Fig. 6. Typically, the mean value will be used to quantify the signal; however, since vibrations are across a fixed position, the mean value in the signal is zero. Therefore, each cut was characterized using the rms value of vibrations during the cutting region, which represent the vibration magnitude on an average sense over the course of cutting. A higher vibration can lead to poor surface quality as well as incidental tool damage (not just wear). As the results show, there is not much difference among all the samples except for Ti-

AM samples, where the magnitude as well as the variation among the samples are high. Interestingly, Ti-AM shows the least cutting power in the previous section but the highest vibration magnitude here. This can be due to its material inhomogeneity, despite the material being easier to remove (i.e., less cutting power).

On the other hand, the vibrations in Ti-W and Ti-W-SR are similar, and no significant effect of stress relieving is observed. However, stress relieving significantly reduces the vibrations in additively manufactured parts as seen by a considerable reduction both in the magnitude as well as the standard deviation.

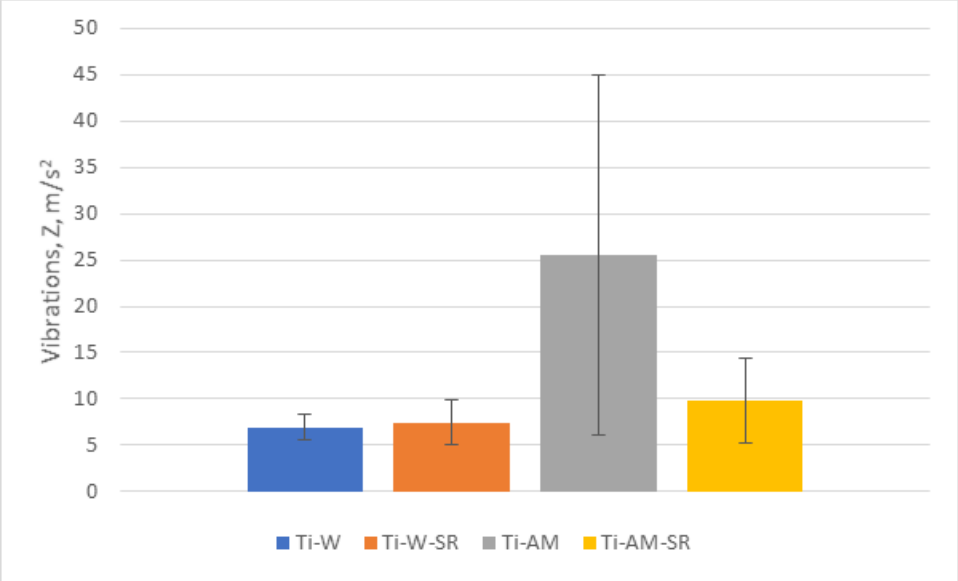

Fig. 6: Dynamic vibration results

3.3 Cutting Zone Temperature Results

The cutting zone temperature was measured, and Fig. 7 shows the results obtained. Overall, the wrought samples tend to produce a slightly higher cutting temperature of about 850°C as compared to their AM counterpart's temperature of about 750°C. The stress-relief heat treatment does not affect the cutting zone temperature though it may alter the material microstructure to a certain extent. Also, although Ti-AM has the lowest cutting power, as shown in Section 3.1, it is not reflected on the cutting temperature, likely due to its higher vibration that contributes additional heat generation.

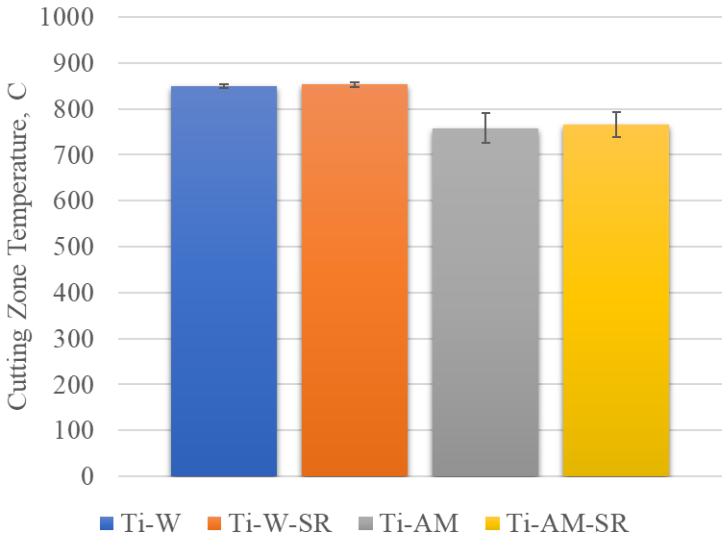

Fig. 7: Cutting zone temperature results

3.4 Surface Roughness Results

The surface roughness values are summarized in Fig. 8. No significant difference in the surface roughness among different materials is observed. All finish cuts reach around 1 μm and below, which are considered a good surface condition. Based on the cutting parameter and tool

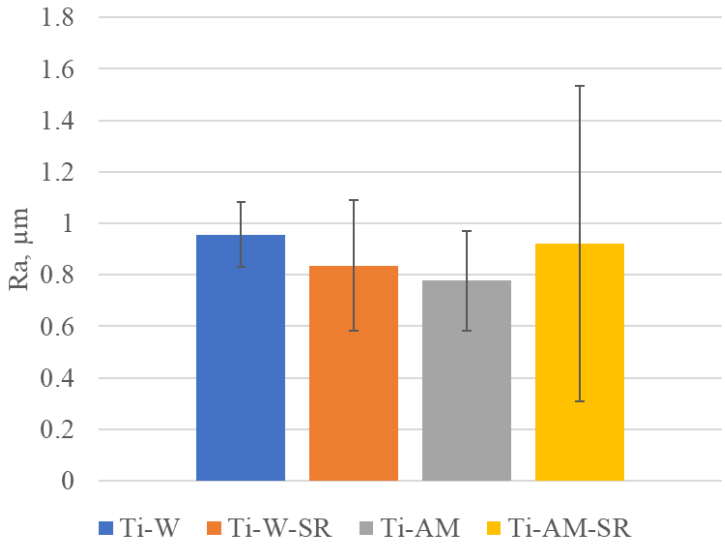

Fig. 8: Surface roughness trend of different materials

nose radius provided, the theoretical surface roughness is 0.8 μm, which matches with the range of the experimental values of all conditions. For a surface finish at this level, the surface is visually smooth, shinning (mirror-like), chatter-free, and the tooling mark is barely seen. Despite a higher vibration magnitude in Ti-AM, that is not reflected on the surface finish, at least under the current cutting condition.

4. Discussion

The machining tests show clear differences between the machinability of wrought samples (Ti-W) and additively manufactured samples (Ti-AM). The cutting power for Ti-W was higher than Ti-AM, while the dynamic vibrations show an opposite trend. This can be explained by their microstructural differences. Ti-6Al-4V is an α+β type alloy containing both hcp (α) and bcc (β) grains. The parts produced using the wrought process have better temperature control throughout the multistep process of manufacturing. Hence wrought parts have a uniform distribution of α and β grains. While the cyclic rapid heating and cooling of the order of $> 10^4$°C /sec in the AM process does not allow enough time for the β grains to form, and therefore, a near α type of Ti alloy is produced. Unlike the wrought part, which is α+β type, the AM parts tend to be near α (α') alloy. This α' type grain structure is martensitic, and the parts produced are brittle due to the titanium-aluminum compound [13]. This is supported by the lower cutting power of Ti-AM compared to Ti-W, but higher vibrations during cutting. It indicates a more brittle microstructure in Ti-AM with small pores/cavities inside the sample or simply the inhomogeneities due to the laser sintering process.

The stress relief process has reduced the vibrations in AM samples but only marginally increased the steady state cutting power. It is possible that the above-mentioned issues are mitigated during the heat treatment in addition to the residual stress. The recommended temperature of 800°C could be high enough to cause recrystallization (annealing) and overall microstructure change. Therefore, the AM parts become more

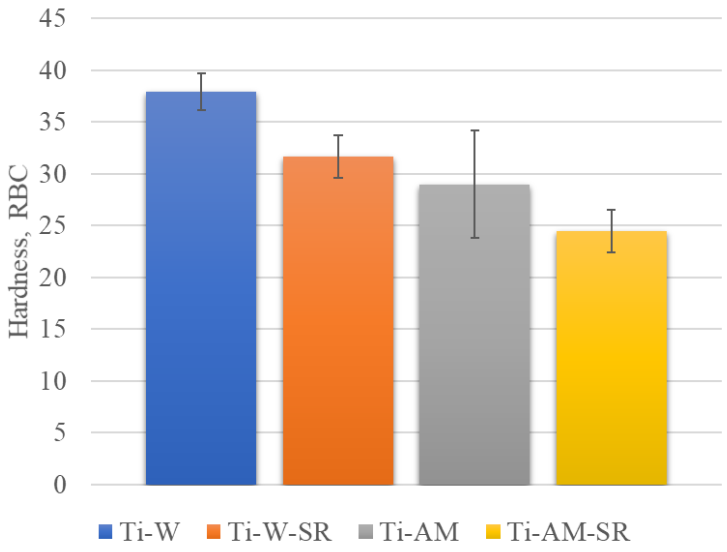

Fig. 9: Rockwell hardness results

homogeneous and ductile after stress relieving. This trend is observed in the data where the steady state cutting power for AM parts increases after stress relieving, but the vibration decreases. Although a thorough microstructure analysis still needs to be conducted, preliminary hardness testing data support these statements. The hardness study was conducted using Wilson Series B2000 Rockwell hardness tester following ASTM E18 standard. As the results shown in Fig. 9,

the heat treatment clearly provides a certain extent of annealing effect on these parts to reduce the hardness, for both wrought (Ti-W) and printed samples (Ti-AM).

On the cutting temperature, it appears that wrought samples (Ti-W and Ti-W-SR) are higher than AM samples (Ti-AM and Ti-AM-SR). This observation is supported by the lower hardness of the AM parts as well as the equal and lower cutting power in the AM parts (Fig. 5). However, it should be noted that cutting temperature is a complicated outcome of material properties, surface condition (i.e., friction), and dynamic events (i.e., vibration), so it cannot be tied to one measurement alone.

In summary, Ti-AM samples have the lowest magnitude of cutting power but the highest vibration magnitude. These vibrations translate directly to dynamic loading and act like impact and fatigue load on the cutting tool and, therefore, can harm the tool more as compared to a steady force. These results aligned with the observation of incidental tool chipping while machining AM parts. Therefore, the cutting parameters for wrought parts may not be used directly on the AM parts. It is also recommended to perform post heat treatment of AM parts to reduce the dynamic load on the tool and machine. The results from the current study did not show any difference between the surface finish of wrought vs. AM parts. One possible reason for this could be because a new cutting tool was used for each test, and the cutting length was also too short to cause tool wear. The cutting speed was another important factor, which had not been investigated at the current scope. All of these will be included in the continuation of this work.

5. Conclusion

This study investigated the machinability of wrought and AM Ti-6Al-4V alloys through machining data (power, temperature, and vibration) and machining outcome (surface roughness). Although a more in-depth microstructure analysis is still needed, it can be concluded from the results that the additively manufactured samples tend to have lower cutting power and more vibration. The behavior may be to the microstructural difference but still requires more analysis to confirm. The post-stress-relief heat treatment can significantly change these phenomena and make the behavior similar to that of wrought material. Tool wear and surface finish do not show noticeable differences at the current cutting condition (e.g., speed, feed, and distance) but are anticipated, given inherent differences of wrought and AM materials based on this study.

Acknowledgments

This work is funded by the Department of Energy's Kansas City National Security Campus, operated by Honeywell Federal Manufacturing & Technologies, LLC, under contract number DE-NA0002839. The authors would also like to thank Dr. Qiang Wu of Kennametal for providing the cutting inserts used in the tests.

References

[1] E. Ezugwu and Z. Wang, "Titanium alloys and their machinability—a review," *J. Mater. Process. Technol.*, vol. 68, pp. 262–274, 1997.

[2] J. Myers, H. Bomberger, and F. Froes, "Corrosion Behavior and Use of Titanium and Its

Alloys," *J. Met.*, vol. 36, pp. 50–60, 2013.

[3] A. Mohammad Hosseini, D. Fraser, S. Masood, and M. Jahedi, "Microstructure and mechanical properties of Ti–6Al–4V manufactured by electron beam melting process," *Mater. Res. Innov.*, vol. 17, pp. s106–s112, 2013.

[4] S. Liu and Y. C. Shin, "Additive manufacturing of Ti6Al4V alloy: A review," *Mater. Des.*, vol. 164, p. 107552, 2019.

[5] M. Despeisse and S. Ford, "The Role of Additive Manufacturing in Improving Resource Efficiency and Sustainability BT - Advances in Production Management Systems: Innovative Production Management Towards Sustainable Growth," in *IFIP International Conference on Advances in Production Management Systems (APMS)*, 2015, pp. 129–136.

[6] Y. Zhai, D. Lados, and J. Lagoy, "Additive Manufacturing: Making Imagination the Major Limitation," *JOM*, vol. 66, pp. 808–816, 2014.

[7] O. Teixeira, L. Pinto Ferreira, and E. Atzeni, "A Review of Heat Treatments on Improving the Quality and Residual Stresses of the Ti–6Al–4V Parts Produced by Additive Manufacturing," *Metals (Basel).*, vol. 10, p. 1006, 2020.

[8] O. Oyelola, D. Crawforth, R. M'Saoubi, and A. Clare, "Machining of Additively Manufactured Parts: Implications for Surface Integrity," 2016.

[9] M. Shunmugavel, A. Polishetty, M. Goldberg, R. Singh, and G. Littlefair, "A comparative study of mechanical properties and machinability of wrought and additive manufactured (selective laser melting) titanium alloy-Ti-6Al-4V," *Rapid Prototyp. J.*, vol. 23, p. 0, Oct. 2017.

[10] G. Rotella, S. Imbrogno, S. Candamano, and D. Umbrello, "Surface integrity of machined additively manufactured Ti alloys," *J. Mater. Process. Technol.*, vol. 259, pp. 180–185, 2018.

[11] J. H. Balaji, V. Krishnaraj, and S. Yogeswaraj, "Investigation on High Speed Turning of Titanium Alloys," *Procedia Eng.*, vol. 64, pp. 926–935, 2013.

[12] D. A. Stephenson, "Tool-Work Thermocouple Temperature Measurement: Theory and Implementation Issues," *J. Eng. Ind.*, vol. 115, pp. 432–437, 1993.

[13] He, Junjie, Duosheng Li, Wugui Jiang, Liming Ke, Guohua Qin, Yin Ye, Qinghua Qin, and Dachuang Qiu. "The martensitic transformation and mechanical properties of Ti6Al4V prepared via selective laser melting." *Materials* 12, no. 2 (2019): 321.